Available online at www.sciencedirect.com
SCIENCE DIRECT®
Wave Motion 43 (2005) 20–28
WAVE MOTION
www.elsevier.com/locate/wavemoti

Finite-amplitude shear wave in pre-stressed thin elastomers

Sia Nemat-Nasser *, Alireza V. Amirkhizi

Center of Excellence for Advanced Materials, Mechanical and Aerospace Engineering, University of California, San Diego, USA

Received 13 April 2005; received in revised form 25 April 2005; accepted 5 May 2005
Available online 17 June 2005

Abstract

We examine the elastic shear waves generated in a thin pre-stressed elastomer layer that is sandwiched between two relatively thick steel plates and is subjected to an elastic shear wave traveling in one of the steel plates. The elastomer layer has been deformed in uni-axial strain in advance, producing in the layer very large axial and lateral compressive stresses of the order of its bulk modulus. Deformations of this kind are produced in the thin layer when the sandwich structure is impacted by another steel plate at an oblique angle. Our results are thus relevant to the analysis of such pressure-shear plate impact experiments.

Keywords: Finite-amplitude shear waves; Pre-stressed elastomers

1. Introduction

Most polymers are elastomeric at temperatures above their glassy transition, T_g. They are solids with very small shear moduli at ordinary pressures and temperatures, but have relatively large bulk moduli. Commercially available polyurethane, for example, is reported by Mott et al. [1] to have a shear modulus of about 6 MPa and a bulk modulus of 2.4 GPa. Similarly, polyurea which is closely related to polyurethane, has a very small shear modulus at room temperature and ordinary pressures, but a relatively large bulk modulus. Elastomers of this kind are *soft solids*, strong in tension and resistant to abrasion and impact. They are commonly used for metal and concrete surface protection. Solids of this kind are fluid-like when they are impacted by high-velocity hard projectiles, but retain their solid-like integrity and regain their initial shape upon the completion of the impact event.

* Corresponding author. Tel.: +1 858 5344914; fax: +1 858 5342727.
E-mail address: sia@ucsd.edu (S. Nemat-Nasser).

0165-2125/$ – see front matter © 2005 Elsevier B.V. All rights reserved.
doi:10.1016/j.wavemoti.2005.05.002

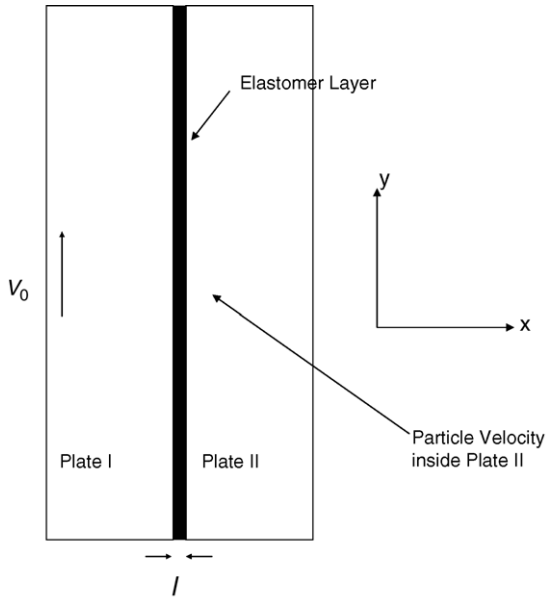

Fig. 1. A thin elastomer layer is sandwiched between two thick steel plates and uni-axially pre-strained. A shear wave with particle velocity V_0 traveling through plate I in the x-direction, impacts the elastomer. The shear velocity at a typical point inside the rear plate is calculated based on the properties of the elastomer.

The shear moduli of elastomers are pressure-dependent, and can reach and exceed 1 GPa when the material is suitably pre-compressed. Confined compression Hopkinson bar and pressure-shear plate impact experiments have been performed to evaluate the pressure-dependence of the shear modulus of elastomers [2,3]. Here, we confine attention to the analysis of shear-wave propagation in a thin layer of an elastomer that is sandwiched between two relatively thick steel plates (Fig. 1), and is pre-deformed in uni-axial strain, producing very large axial and lateral compressive stresses in the thin elastomer.

The problem of finite deformation elastic waves has been studied extensively in the literature, especially for hyper-elastic materials. Truesdell [4] has studied the propagation of small oscillation superposed on large deformations in hyper-elastic materials based on the work by Toupin and Bernstein [5]. Bland [6] has addressed the problem of *simple* waves for which the propagation direction coincides with one of the principal axes of the stress or deformation tensors. Chu [7] has discussed wave propagation in incompressible materials. Truesdell [8,9] has introduced the concept of hypo-elasticity and shortly afterwards Noll [10] has shown that it encompasses the Cauchy elasticity. Bernstein [11] found the necessary and sufficient conditions for a hypo-elastic material to be elastic in the sense of Cauchy and even furthermore in the sense of Green (hyper-elasticity). It is now well established that this general framework is a natural choice for most numerical routines and can be extended to plasticity and other material properties [12]. Truesdell [8,9,13] has solved a few simple problems using this model. More recently, Lin et al. [14] have studied uniform quasi-static deformation in a closed path, which includes uniform simple shearing, for several hypo-elastic material models.

In the present work, we use a hypo-elastic model based on a linear relation between the Jaumann rate of the Cauchy stress and deformation rate tensors. As is known, models based on other objective stress rates and material strain rates can be rendered equivalent by proper selection of the tangential moduli; for a discussion of this equivalence see Nemat-Nasser [15].

2. Analysis

The coordinate system is shown in Fig. 1. We assume that the uni-axial pre-strain results in the following uniform strains and stresses in the elastomer layer:

$$\varepsilon_{yy} = \varepsilon_{zz} = 0 \tag{1}$$

$$\varepsilon_{kk} = \varepsilon_{xx} \tag{2}$$

$$\sigma_{xx} = 2G\left(\varepsilon_{xx} - \frac{\varepsilon_{kk}}{3}\right) + K\varepsilon_{kk} = \left(K + \frac{4G}{3}\right)\varepsilon_{xx} \tag{3}$$

$$\sigma_{yy} = \sigma_{zz} = 2G\left(\varepsilon_{yy} - \frac{\varepsilon_{kk}}{3}\right) + K\varepsilon_{kk} = \left(K - \frac{2G}{3}\right)\varepsilon_{xx} \tag{4}$$

Here, K and G are the bulk and shear moduli of the elastomer layer, respectively. For finite deformations, a linear relation between the strain and the Cauchy stress components does not generally hold. However, the above results can be derived from the hypo-elastic constitutive relation if one uses the logarithmic strain; see Appendix A. Therefore, prior to the arrival of the shear wave, the stress components are assumed to be uniform, having the following values:

$$\sigma^0_{xx} = -p \tag{5}$$

$$\sigma^0_{yy} = \sigma^0_{zz} = -\frac{3K - 2G}{3K + 4G}p \tag{6}$$

where σ^0_{xx} is the axial stress, σ^0_{yy} and σ^0_{zz} are the confining stresses and p is the axial pressure.

The thin layer is now subjected to a simple shearing by an elastic shear wave that travels in the steel plate I in Fig. 1, and transmits an initial particle velocity, V_0, to the layer at its face in contact with the plate. With the pre-stressed configuration taken as the reference one (X, Y, Z), the shearing motion is expressed as:

$$x = X \tag{7}$$

$$y = Y + v(t, X) \tag{8}$$

$$z = Z \tag{9}$$

$$\frac{\partial v}{\partial X} = \gamma \tag{10}$$

where (x, y, z) define the current particle position. The deformation rate and spin tensors are:

$$\boldsymbol{D} = \frac{\dot\gamma}{2}(e_x \otimes e_y + e_y \otimes e_x) \tag{11}$$

$$\boldsymbol{W} = \frac{\dot\gamma}{2}(e_y \otimes e_x - e_x \otimes e_y) \tag{12}$$

Now assume an incremental hypo-elastic constitutive model (see Appendix A for details), where the Jaumann rate of the shear stress is given by:

$$\overset{\circ}{\tau}(= \overset{\circ}{\sigma}_{xy}) = 2GD_{xy} = G\dot\gamma \tag{13}$$

The stress rate is calculated from:

$$\dot\sigma = \overset{\circ}{\sigma} + \mathbf{W}\sigma + \sigma\mathbf{W}^{\mathrm{T}} \tag{14}$$

Since the shear component is the only non-zero element of the deformation rate tensor, the non-zero components of the stress rate tensor are:

$$\dot{\sigma}_{xx} = -\dot{\gamma}\tau = -\dot{\sigma}_{yy} \tag{15}$$

$$\dot{\tau} = \left(G + \frac{\sigma_{xx} - \sigma_{yy}}{2}\right)\dot{\gamma} \tag{16}$$

From equilibrium, the shear-wave speed and impedance then are:

$$c = \sqrt{\frac{\mathrm{d}\tau/\mathrm{d}\gamma}{\rho}} \tag{17}$$

$$z = \sqrt{\rho\frac{\mathrm{d}\tau}{\mathrm{d}\gamma}} \tag{18}$$

The quantity ρ here is the mass density of the compressed elastomer layer. Define a new quantity, ξ, and eliminating γ, obtain:

$$\xi = \frac{\sigma_{xx} - \sigma_{yy}}{2} \tag{19}$$

$$\dot{\xi} = \dot{\sigma}_{xx} = -\dot{\sigma}_{yy} \tag{20}$$

$$\dot{\gamma} = -\frac{1}{\tau}\dot{\xi} \tag{21}$$

Replace in the differential equation for τ and solve for ξ:

$$\xi = \sqrt{(G + \xi(0))^2 - \tau^2} - G \tag{22}$$

$$\dot{\tau} = \sqrt{(G + \xi(0))^2 - \tau^2}\,\dot{\gamma} \tag{23}$$

The complete solution and the apparent tangential shear stiffness needed in wave propagation calculation can now be written down as follows:

$$\tau = C\sin\gamma \tag{24}$$

$$\xi = C\cos\gamma - G \tag{25}$$

$$\sigma_{xx} = -p - C(1 - \cos\gamma) \tag{26}$$

$$\sigma_{yy} = -p\frac{3K - 2G}{3K + 4G} + C(1 - \cos\gamma) \tag{27}$$

$$\frac{\mathrm{d}\tau}{\mathrm{d}\gamma} = C\cos\gamma \tag{28}$$

$$C = (G + \xi(0)) = G - p\frac{6G}{4G + 3K} \tag{29}$$

Note that there is no restriction on the history of γ in this derivation. The equilibrium equation:

$$\frac{\partial^2 v}{\partial t^2} - \frac{1}{\rho}\frac{\partial \tau}{\partial x} = 0 \tag{30}$$

is rewritten in light of the above result as follows:

$$\frac{\partial \tau}{\partial x} = \frac{\mathrm{d}\tau}{\mathrm{d}\gamma}\frac{\partial \gamma}{\partial x} = C\cos\left(\frac{\partial v}{\partial x}\right)\frac{\partial^2 v}{\partial x^2} \tag{31}$$

$$\frac{\partial^2 v}{\partial t^2} - \frac{C}{\rho}\cos\left(\frac{\partial v}{\partial x}\right)\frac{\partial^2 v}{\partial x^2} = 0 \tag{32}$$

Eq. (32) can be solved numerically by discretizing the layer through the thickness. The boundary conditions can be derived from the continuity of the displacement (or equivalently velocity) and the tractions at the interface between the steel plates and the layer. We consider both no-slip and possible slip conditions at the front interface, but only a no-slip condition at the rear interface. For the rear plate II, therefore, these boundary conditions written at $x = \mathrm{l}$ are,

$$v^{\mathrm{m}}(l,t) = v^{\mathrm{p}}(l,t), \qquad \tau^{\mathrm{m}}(l,t) = \tau^{\mathrm{p}}(l,t) \Rightarrow \frac{\partial v^{\mathrm{m}}(l,t)}{\partial t} = \frac{C}{\sqrt{\rho_{\mathrm{p}} G_{\mathrm{p}}}}\sin\left(\frac{\partial v^{\mathrm{m}}(l,t)}{\partial x}\right) \tag{33–35}$$

Here, the superscript or subscript p denotes the plate and m denotes the elastomer layer.

At the front end $x = 0$ one needs to take into account the incoming wave and its reflection. The incoming wave has a particle velocity of V_0. For the no-slip case, we have,

$$\begin{aligned} &v^{\mathrm{m}}(0,t) = v^{\mathrm{p}}(0,t) \Rightarrow \frac{\partial v^{\mathrm{m}}(0,t)}{\partial t} = V_0 + \frac{\partial v^{\mathrm{r}}(0,t)}{\partial t} \\ &\tau^{\mathrm{m}}(0,t) = \tau^{\mathrm{p}}(0,t) \Rightarrow \tau^{\mathrm{m}}(0,t) = \sqrt{\rho_{\mathrm{p}} G_{\mathrm{p}}}\left(V_0 - \frac{\partial v^{\mathrm{r}}(0,t)}{\partial t}\right) \\ &\frac{\partial v^{\mathrm{m}}(0,t)}{\partial t} = 2V_0 - \frac{C}{\sqrt{\rho_{\mathrm{p}} G_{\mathrm{p}}}}\sin\left(\frac{\partial v^{\mathrm{m}}(0,t)}{\partial x}\right) \end{aligned} \tag{36–40}$$

Here the superscript r denotes the wave reflected back into the steel plate.

The boundary conditions ((33), (35), (36) and (40)), imposed on the elastomer layer, implicitly exclude reflections from the free surfaces of the steel plates I and II. Multiple reflections from the interfaces between the elastomer and the steel plates are, however, included, as these are essential parts of the dynamic response of the elastomer. But, since the thicknesses of the steel plates are considerably larger than that of the elastomer layer, the reflections off their free surfaces can be safely neglected during the initial phases of the deformation of the elastomer. Note, however, that the particle velocity on the free surface of the rear plate II is given by $2\partial v^{\mathrm{p}}(l,t)/\partial t$.

The above formulation is applicable when the material is strong enough to bear the stresses and strains produced at the interface with the steel plates. Various ad hoc and phenomenological failure conditions may be introduced in the numerical simulation to model potential interface and material degradation. In this work, in addition to the above-mentioned no-slip boundary conditions, we considered for illustration two cases. First, we study the effect of potential frictional slip that is idealized by an interface, which can support only up to a constant critical shear stress. The results also apply to a case when the layer can only support up to a constant shear stress, say, τ_{c} after which the transmitted shear stress through the elastomer remains constant at τ_{c}. Second, we use a progressively degrading material whose stiffness decays exponentially with the shear straining,

$$C(\gamma) = C(0)\,\mathrm{e}^{-\alpha\gamma} \tag{41}$$

Here,α is a dimensionless parameter that idealizes the intensity of the material degradation by, say, void nucleation and micro-shearbanding produced by shearing.

Table 1
Dimensionless values used in numerical calculations

$\bar{G}$	1/3, 1/2, 1
$\bar{K}$	10
$\bar{\rho}$	0.000125
$\bar{G}_{\mathrm{p}}$	30
$\bar{\rho}_{\mathrm{p}}$	0.001

3. Examples

We now consider illustrative numerical examples. All the parameters are rendered dimensionless using the pre-existing axial pressure, p, initial particle velocity in steel, V_0, and the elastomer layer thickness, l. The other parameters are selected in a way to reproduce an experiment for a thin layer of soft nearly incompressible rubber-like material, sandwiched between two high-density and stiff steel plates. We thus set,

$$\bar{G} = \frac{G}{p}, \qquad \bar{K} = \frac{K}{p}, \qquad \bar{\rho} = \frac{\rho V_0^2}{p}, \qquad \bar{G}_{\mathrm{p}} = \frac{G_{\mathrm{p}}}{p}, \qquad \bar{\rho}_{\mathrm{p}} = \frac{\rho_{\mathrm{p}} V_0^2}{p} \tag{42–46}$$

Here G, K and ρ are, respectively, the shear modulus, bulk modulus and the density of the elastomer in the pre-stressed condition, while G_{p} and ρ_{p} are the shear modulus and density of the front and rear plates. The value of the bulk modulus K is needed in order to calculate the stiffness parameter C. Three different values for the normalized shear stiffness are used to illustrate the effect of shear stiffness on the resulting wave propagation. Table 1 gives the values of the parameters used in the numerical examples.

A simple and straightforward dynamic finite-element method is used for the numerical calculations. The thickness of the elastomer is divided into N equal elements. The central-difference method is used for the time discretization. The time-step is checked to ensure that it is smaller than the time required for the wave to travel through one element, i.e., smaller than the critical time-step [16]. The boundary conditions are enforced using (35) and (40), which require calculation of the stress only inside the elastomer. The steel plates are linearly elastic with small displacement and velocity. Hence, their velocities at any interior point are easily related to those at the interface with the elastomer. In fact, neglecting the dispersion, the displacement at an interior point of plate II is merely a time shift of that at its interface with the elastomer layer. The results of this scheme are also compared with those obtained using a method that extends the finite-element calculation into boundary layers inside the steel plates and decomposes the wave into incoming and reflected components, arriving at essentially the same results to within the numerical errors; therefore, these results are not presented here. Even though, in reality, release waves do reflect off the free surfaces of the steel plates and return back to the interface with the elastomer, affecting the subsequent response of the sandwich structure, for clarity, we do not include these in what follows, assuming that the steel plates are very thick relative to the thickness of the elastomer layer.

4. Discussion

The graphs in Fig. 2 show the normalized particle velocity (divided by V_0) versus normalized time (divided by l/V_0), at a typical point near the interface inside the rear plate II; the high frequency oscillation at the beginning of each step is an artifact of the numerical method used. In the absence of release waves, this velocity should approach the initial particle velocity, V_0, if there is no slip at the interfaces, or other material degradation. The time that it takes to achieve this final velocity, however, will depend on the magnitude of the effective shear modulus of the elastomer.

To examine the effect of the pre-stress on the shear-wave propagation, we have given in Fig. 3 the corresponding solution which uses the actual shear modulus, $G = p/3$, instead of the apparent shear modulus, C, that reflects the

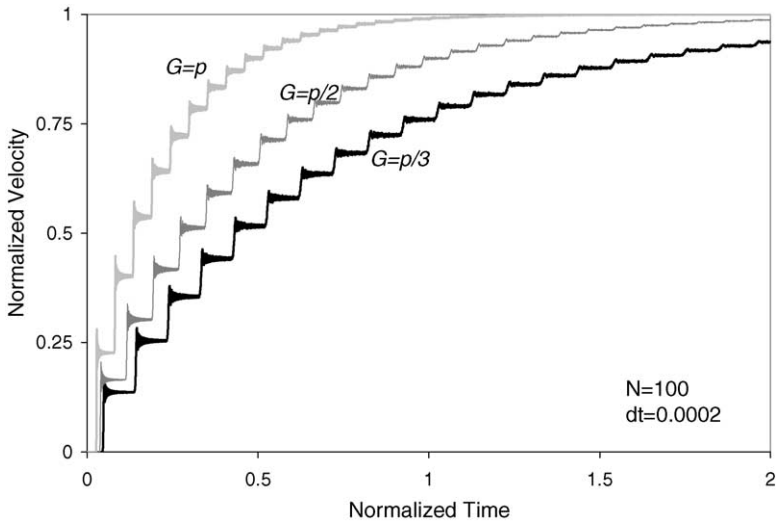

Fig. 2. Normalized particle velocity (velocity/V_0) in the rear plate for indicated values of the shear modulus, G. In the absence of release waves reflecting off the free faces of the steel plates, the final velocity would approach V_0 regardless of the value of the shear modulus, if there is no interface slip or other material failure. Normalized time = actual time/(l/V_0).

presence of the axial and lateral stresses, as is detailed in the preceding sections. Therefore, even for a simple constitutive relation such as hypo-elasticity, the pre-stress effect can modify the wave propagation results. Hence, when extracting the material parameters from the results of this kind of impact experiment, it is necessary to include the effect of the pre-stresses in order to obtain relevant and unambiguous results.

If interface or other failure occurs in the elastomer, the stress wave transmitted through the elastomer layer will be limited in magnitude and the maximum velocity observed inside of the plate II will be less than V_0. Two ad hoc models are used to illustrate the effect of such failure on the wave propagation; see Fig. 4. Perfect yielding (or slip) abruptly renders the transferred velocity a constant that can be related to the yield stress, τ_c through the impedance

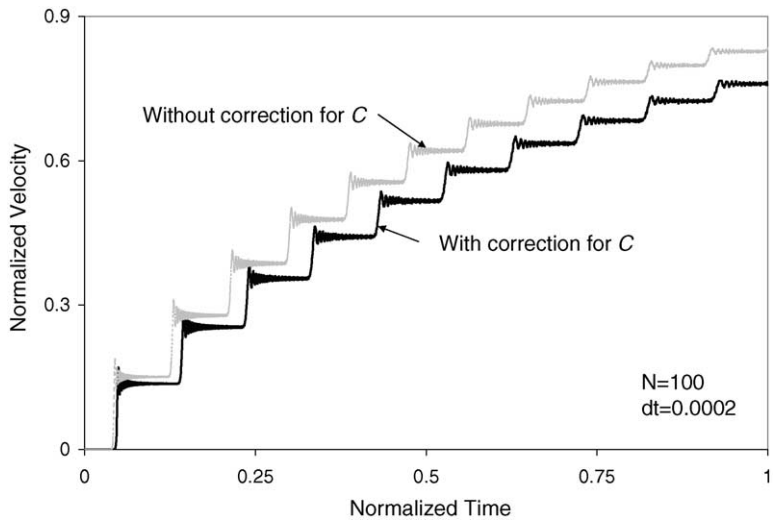

Fig. 3. Effect of correction in the value of C due to pre-stress.

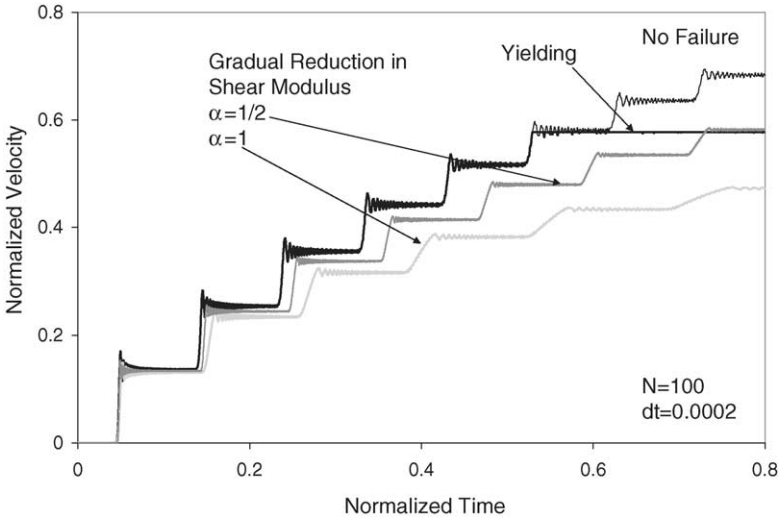

Fig. 4. Effect of stiffness degradation or yielding (interface slip) on the rear plate particle velocity.

of the elastomer layer; this is illustrated in Fig. 4 for $\tau_c/p = 0.1$ The progressive failure does not show this abrupt behavior, as is seen from the results for $\alpha = 1/2.1$.

Acknowledgements

The authors wish to express thanks to Prof. Rod Clifton and his graduate student Tonia Jiao for sharing with us their results on pressure-shear experiments of thin layers of polyurea. This work was supported by ONR N00014-03-M-0172 under Dr. Roshdy Barsoum's Program.

Appendix A

Here we show that Eqs. (3) and (4) are compatible with a hypo-elastic constitutive relation that also collapses to (13) for simple shearing. This constitutive equation is given by:

$$\overset{\circ}{\sigma} = K\,\mathrm{tr}(\mathbf{D})\mathbf{1}^{(2)} + 2G\left(\mathbf{D} - \frac{\mathrm{tr}(\mathbf{D})}{3}\mathbf{1}^{(2)}\right) \tag{47}$$

where $\mathbf{1}^{(2)}$ is the second-order identity tensor. For uni-axial straining, as described in (1) and (2), one has:

$$\mathbf{W} = 0 \Rightarrow \dot{\sigma} = \overset{\circ}{\sigma}, \qquad \mathbf{D} = \frac{\dot{\lambda}}{\lambda} e_x \otimes e_x \tag{48–50}$$

Here, λ is the principal stretch in the loading direction. Therefore, one may write,

$$\dot{\sigma} = \frac{\dot{\lambda}}{\lambda}\left[\left(K + \frac{4G}{3}\right) e_x \otimes e_x + \left(K - \frac{2G}{3}\right)(e_y \otimes e_y + e_z \otimes e_z)\right] \tag{51}$$

and upon integration obtain,

$$\sigma = \varepsilon_{xx}\left[\left(K + \frac{4G}{3}\right)(e_x \otimes e_x) + \left(K - \frac{2G}{3}\right)(e_y \otimes e_y + e_z \otimes e_z)\right] \tag{52}$$

This is equivalent to (3) and (4) when we use the logarithmic strain.

References

[1] P.H. Mott, C.M. Roland, R.D. Corsaro, Acoustic and dynamic mechanical properties of a polyurethane rubber, J. Acoust. Soc. Am. 111 (2002) 1782–1790.
[2] S. Nemat-Nasser, A.V. Amirkhizi, J. Isaacs, Experimental Characterization of Polyurea, CEAM Technical Report to ONR, December 2003.
[3] R.J. Clifton, T. Jiao, High strain rate response of elastomers, in: Presentation to ERC ACTD Workshop, Cambridge, MA, November 2004.
[4] C. Truesdell, General and exact theory of waves in finite elastic strain, Arch. Rational Mech. Anal. 8 (1961) 263–296.
[5] R.A. Toupin, B. Bernstein, Sound waves in deformed perfectly elastic materials. Acoustoelastic effect, J. Acoust. Soc. Am. 33 (1961) 216–225.
[6] D.R. Bland, Nonlinear Dynamic Elasticity, Blaisdell, Waltham, MA, 1969.
[7] B.-T. Chu, Finite amplitude waves in incompressible perfectly elastic materials, J. Mech. Phys. Solids 12 (1964) 45–57.
[8] C. Truesdell, The mechanical foundations of elasticity and fluid dynamics, J. Rational Mech. Anal. 1 (1952) 125–300.
[9] C. Truesdell, Corrections and additions to the mechanical foundations of elasticity and fluid dynamics, J. Rational Mech. Anal. 2 (1953) 595–616.
[10] W. Noll, On the continuity of the solid and fluid states, J. Rational Mech. Anal. 4 (1955) 3–81.
[11] B. Bernstein, Hypo-elasticity and elasticity, Arch. Rational Mech. Anal. 6 (1960) 89–104.
[12] R.J. Clifton, Plastic waves: theory and experiment, in: S. Nemat-Nasser (Ed.), Mech. Today, vol. 1, Pergamon, New York, 1974, pp. 102–167.
[13] C. Truesdell, Hypo-elastic shear, J. Appl. Phys. 27 (1961) 441–447.
[14] R.C. Lin, U. Schomburg, T. Kletschkowski, Analytical stress solutions of a closed deformation path with stretching and shearing using the hypoelastic formulations, Eur. J. Mech. A Solids 22 (2003) 443–461.
[15] S. Nemat-Nasser, Plasticity: A Treatise on Finite Deformation of Heterogeneous Inelastic Materials, Cambridge University Press, Cambridge, UK, 2004.
[16] T.J.R. Hughes, The Finite Element Method: Linear Static and Dynamic Finite Element Analysis, Dover, Mineola, NY, 2000.